 doi:10.20944/preprints201807.0444.v1

Article

Low Order Harmonics Control in Stair Case Waveform by a Novel Estimation based Technique

Salman Ahmad[1], Atif Iqbal[2], Imtiaz Ashraf[1], Sanjeevikumar Padmanaban[3,*], Mohammed Meraj[2]

[1] Department of Electrical Engineering, Aligarh Muslim University, Aligarh, India; salmanahmad19@gmail.com, iashraf@rediffmail.com
[2] Department of Electrical Engineering, Qatar University, Qatar; atif.iqbal@qu.edu.qa, meraj@qu.edu.qa
[3] Department of Energy Technology, Aalborg University, 6700 Esbjerg, Denmark; san@et.aau.dk
* Correspondence: san@et.aau.dk; Tel.: +45-71-682-084

Abstract: Few switching transitions in high power and medium voltage application of Power converters are desirable. The selective harmonics elimination (SHE) pulse width modulation offers a better quality waveform with lower switching transitions and hence lower switching losses. The SHE is a pre-programmed modulation technique where certain amounts of lower order harmonics are removed and fundamental voltage is controlled. After Fourier analysis of output waveform, a set of nonlinear transcendental equations is obtained which exhibits, multiple, unique or no solution in different range of modulation index (MI). In this paper, an iterative method based on the Jacobian estimate is proposed to solve a highly non-linear set of SHE equations. The proposed technique is easy in implementation and can solve a large number of such equations as computation of the Jacobian matrix in the subsequent iteration is estimated from the previous values. Moreover, the proposed method also removes the singularity problem, especially for large SHE equations. High accuracy in the initial guess is also not essential for this method and can converge to the solution with any random initial guess. The computational and simulation results are given to validate the concept. The hardware result is provided to confirm the computational and simulation results.

Keywords: Staircase Waveform; Harmonics Control; Field Programming gate array (FPGA); Estimation; Iterative technique, VHDL

1. Introduction

Multilevel voltage source/current source converters have been widely studied and researched for a variety of applications which includes induction machine drives, renewable energy integration in the grid, active rectifiers, pumps, fans, rolling mills, marine propulsion, HVDC transmission, railway traction etc. [1–7]. Various research groups mainly focused on its topology, modulation, and control algorithm. The important topologies include Neutral point clamped (NPC), cascaded H bridge (CHB) and Flying capacitor (FC) and various hybrid topologies such as active neutral point clamped (ANPC), H bridge neutral point clamped (HNPC) etc. The performance characteristics of multilevel converters are highly dependent on the choice of modulation techniques adopted for their operation. The broad classification of important modulation techniques is high switching frequency pulse width modulation techniques and low switching frequency techniques [8]. The high switching frequency techniques include sine pulse width modulation (SPWM) based phase shifted (PS-PWM), level shifted (LS-PWM) and space vector pulse width modulation (SVPWM) [3]. The low switching frequency modulation techniques are classified as optimum PWM, selective harmonics elimination (SHE) PWM, nearest vector control (NVC) PWM and selective harmonics mitigation (SHM) PWM [9-10]. In the high switching frequency PWM techniques the power

Preprints (www.preprints.org) | NOT PEER-REVIEWED | Posted: 24 July 2018 doi:10.20944/preprints201807.0444.v1

switches are operated at several kHz and yield good quality waveforms whereas lower switching frequency PWM techniques operate power electronics switches at few hundreds of Hertz [11–12].A detailed classification modulation method for the multi-level inverter is shown in Fig.1 [3], [8], [10].

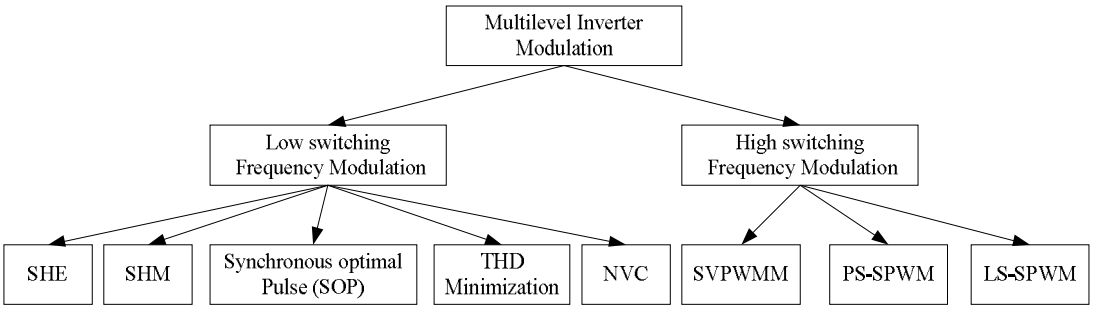

Figure 1. Pulse width modulation techniques for multilevel inverter

In medium voltage and high power converters, low switching frequency PWM techniques are preferred as the switching losses are one of the most important criteria for its operation. Among various low switching frequency PWM techniques, SHE PWM is widely investigated and researched for various industrial applications [11–14], [15–20]. It is a pre-programmed PWM technique which selectively eliminates particular harmonics along with control of the fundamental voltage [21–26]. The Fourier series analysis of the output waveform is carried out and set of nonlinear transcendental equations are obtained which eliminates pre-specified order of harmonics along with control of the fundamental frequency voltage component. After offline computation for switching angles is done, these values for the different modulation index are stored in a look-up table [27]. Depending upon the modulation index a particular set of switching angles applies to the power electronics switches in order to obtain the desired waveform at the output. Some literature also tried to implement it in real times by adopting techniques such as artificial neural network (ANN), model predictive control, and criteria based control techniques [28–31]. Real-time implementation is useful, especially in unequal dc voltages such as application in solar photovoltaic as the size of the lookup table is huge and will consume a lot of memory of the processor board. A criteria based modulation (CBM) strategy is also proposed which selects the optimum switching angles from a given objective function while considering all the practical constraints such as minimum ON and OFF times from the set of solution stored in the lookup table[32].

The main challenge to utilize SHE modulation methodology lies in solving the switching angles from the set of nonlinear transcendental equations which exhibits unique, multiple or no solution for different values of modulation indices (MI). The most commonly used methods to solve these equations proposed in the literature are the numerical techniques based conventional methods, Algebraic methods and various optimization methods such evolutionary and swarm-based metaheuristic methods. The numerical based methods mainly include Newton Raphson method, sequential homotopy and analytical methods [23],[33–34]. Numerical methods are very simple to use, but an accurate guess along with computation of derivates makes these methods difficult to use and sometimes may fail to give all the solution to the problem. Moreover, they are useful to solve only few switching angles as calculation of first derivatives become very difficult as size increases. Algebraic methods such as Walsh function, resultant theory, and Groebner method are proposed in [35-37]. In the algebraic method, the trigonometric equations are first converted into polynomial equations by multiple angle formulas and then are solved by a simple Gaussian elimination method of solving linear equations. Although these methods can give all the possible solutions, but as the

Preprints (www.preprints.org) | NOT PEER-REVIEWED | Posted: 24 July 2018 doi:10.20944/preprints201807.0444.v1

number of switching angle increases more than four, the method becomes very complex and time-consuming. The optimization based methods such as genetic algorithm (GA)[38], particle swarm optimization (PSO)[39], Bee algorithm[40], ant colony optimization (ACO)[41], memetic algorithm [42] and differential evolution (DE) algorithm[27], tries to minimize an objective function to obtain optimal switching angles. Although the optimization method is less dependent on initial guess, but is very slow convergent, doesn't give very accurate results and takes longer time in its computation. Moreover, it requires an experience and expert knowledge of its computational algorithm. A detailed analysis of various optimizations based SHE methods is given in [10], [43].

In this paper, a novel iterative method with Jacobian estimates is proposed. The proposed method is fast convergent and easier in its implementation. Moreover, it gives all the possible solutions with any random, initial guess which overcomes the problem of numerical techniques. Also, the proposed method is capable of evaluating a large number of switching angles (levels) with efficient convergence. The computational results are presented for various switching angles starting from five switching angles (11-levels) to fifteen switching angles (31-level). The harmonics profile at some particular modulation index and %THD is also given. The simulation results of phase and line voltages are obtained using Simulink to verify the computational results. A prototype is also built in the laboratory to validate the computational and simulation results.

2. Problem Formulation: Mathematical Analysis

Figure 2a shows a typical configuration of single phase cascaded H-cell inverter having n cells with n- separate dc sources. The IGBT switches operated in the fundamental switching frequency. The output voltage of the cascaded H Bridge is given by the summation of voltages from different H-cells. To analyze the output voltage waveform from the inverter, Fourier series expansion is used. The general Fourier series expansion can be expressed as (1);

$$v(\alpha) = \frac{a_0}{2} + \sum_{n=1}^{\infty} a_n \cos(n\alpha) + b_n \sin(n\alpha) \tag{1}$$

Where Fourier Coefficients are defined as (2) and (3)

$$a_n = \frac{1}{\pi}\int_{-\pi}^{\pi} v(\alpha)\cos(n\alpha)d\alpha\,, \quad n \geq 0 \tag{2}$$

$$b_n = \frac{1}{\pi}\int_{-\pi}^{\pi} v(\alpha)\cos(n\alpha)d\alpha\,, \quad n \geq 1 \tag{3}$$

Considering quarter wave symmetry in the output waveform shown in Fig. 2b, we will have $a_0=0$ and $a_n=0$ and the generalized Fourier coefficient for the multilevel stepped waveform is given by (4).

$$b_n = \begin{cases} \dfrac{4V_{dc}}{n\pi}\displaystyle\sum_{k=1}^{N_s}\cos(n\alpha_k)\,, & for\ odd\ n \\ 0\,, & for\ even\ n \end{cases} \tag{4}$$

Where b_n is the amplitude of the n^{th} harmonics and N_s is the number of switching angles in a quarter's period. By having N_s switching angles in a quarterly period N_s-1 harmonics can be eliminated along with control of the fundamental frequency component, defined by modulation index,

Preprints (www.preprints.org) | NOT PEER-REVIEWED | Posted: 24 July 2018 doi:10.20944/preprints201807.0444.v1

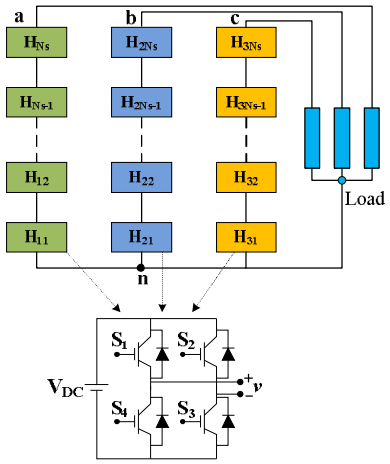

(**a**)

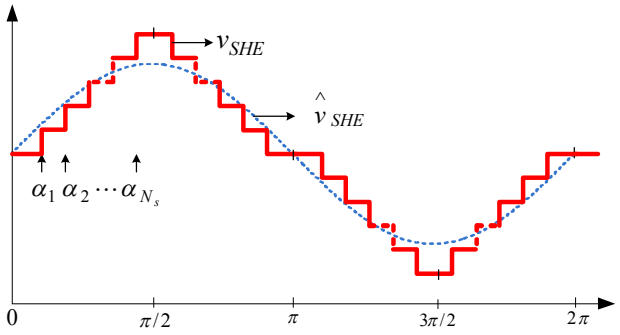

(**b**)

Figure2. Generalized multilevel inverter structure**(a)** Circuit topology**(b)** Output stepped waveform from one leg

m (0<m<1). The set of non-linear transcendental equations is given by (5) and (6) while eliminating lower order harmonics along with varying *m* in linear range.

$$m \times N_s = \frac{4V_{dc}}{\pi} \sum_{k=1}^{N_s} \cos(\alpha_k) \tag{5}$$

$$0 = \sum_{k=1}^{N_s} \cos(n\alpha_k) \tag{6}$$

Where $n \in \{3,5,7 \cdots 2N_s+1\}$ in the case of single phase cascaded H-bridge inverter and for 3 phase case $n \in \{5,7,11,13 \cdots 3N_s-2\,;\, N_s\ odd\}$ or $n \in \{5,7,11,13 \cdots 3N_s-1\,;\, N_s\ even\}$ .The amplitude of the fundamental frequency component for both the cases is given by (7).

$$\hat{v}_{SHE,1} = \frac{4V_{dc}mN_s}{\pi} \tag{7}$$

Where $\hat{v}_{SHE,1}$ is defined as the fundamental frequency voltage magnitude. In the case of five switching angles (11-level), the set of selective harmonic elimination equations for 3-phase multilevel inverter considering four low order non-triplen harmonics for elimination is given in (8)

Preprints (www.preprints.org) | NOT PEER-REVIEWED | Posted: 24 July 2018 doi:10.20944/preprints201807.0444.v1

$$G=\begin{bmatrix}\cos(\alpha_1)+\cos(\alpha_2)+\cos(\alpha_3)+\cos(\alpha_4)+\cos(\alpha_5)-5m\\ \cos(5\alpha_1)+\cos(5\alpha_2)+\cos(5\alpha_3)+\cos(5\alpha_4)+\cos(5\alpha_5)\\ \cos(7\alpha_1)+\cos(7\alpha_2)+\cos(7\alpha_3)+\cos(7\alpha_4)+\cos(7\alpha_5)\\ \cos(11\alpha_1)+\cos(11\alpha_2)+\cos(11\alpha_3)+\cos(11\alpha_4)+\cos(11\alpha_5)\\ \cos(13\alpha_1)+\cos(13\alpha_2)+\cos(13\alpha_3)+\cos(13\alpha_4)+\cos(13\alpha_5)\end{bmatrix} \quad (8)$$

The generalized non-linear transcendental equation given in (5) and (6) for various cases is solved in the next section by using the proposed Jacobian estimation based iterative technique.

3. Switching Angles Computation by Fast Novel approach

The selective harmonics elimination represents a set of n non-linear simultaneous transcendental equations, having equality and non-equality constraints with maximum and minimum bounds on the design variables, which in generalized and vector form is represented by (9), and (10).

$$\begin{aligned}&Solve\ G(\alpha)\approx 0\\ &subject\ to\\ &\quad g_k(\alpha)\le 0,\quad k=1,2,\cdots M\\ &\quad h_t(\alpha)=0,\quad t=1,2,\cdots T\\ &\quad L^i\le\alpha^i\le U^i,\quad i=1,2,\cdots N\end{aligned} \quad (9)$$

$$\Omega=\left\{\begin{matrix}\alpha=[\alpha_1,\alpha_2,\alpha_3,\cdots\alpha_{Ns}]\in R^N\,|\,g_k(\alpha)\le 0,h_t(\alpha)=0,\\ L^i\le\alpha_i\le U^i\ \forall\ i\in\left(1,\bar{N_s}\right)\end{matrix}\right\} \quad (10)$$

Where $\alpha\in R^n$ and $G(\cdot):R^n\to R^n$ is a $n\times1$ function matrix. This problem may have many, unique or no solution. The inequality along with upper and lower bounds on the switching angles is given by (11).

$$0\le\alpha_1\le\alpha_2\le\alpha_3\cdots\le\alpha_{Ns}\le\frac{\pi}{2} \quad (11)$$

In the Newton Raphson method, the main challenge is in the computation of the Jacobian matrix in the subsequent iterations. This problem further aggravated in solving the nonlinear equation for large variables. In addition, the Jacobian Matrix becomes a singular matrix when the difference in the solution vectors in the consecutive iterations becomes small. These challenges can be solved be adopting a technique which needs Jacobian matrix computation only at the start of the algorithm and then Jacobian matrix in the subsequent iterations is estimated using previous iteration values. At the start of the algorithm, the initial values of different functions are obtained using (12) to (14).

$$\boldsymbol{J}^{(0)}=\left[\frac{\partial\boldsymbol{G}(\boldsymbol{\alpha}^{(0)})}{\partial\boldsymbol{\alpha}}\right] \quad (12)$$

$$\Delta\boldsymbol{\alpha}^{(i)}=-\left[\boldsymbol{J}^{(0)}\right]^{-1}\boldsymbol{G}^{(i)} \quad (13)$$

$$\boldsymbol{\alpha}^{(i+1)}=\boldsymbol{\alpha}^{(i)}+\Delta\boldsymbol{\alpha}^{(i)} \quad (14)$$

The value of Jacobian Matrix in (12) alternatively can be estimated by using the values of function vectors evaluated in the previous iterations. If moving from i^{th}iteration to $(i+1)^{th}$ iteration the difference in solution vectors is not large, then the Jacobian matrix in the $(i+1)^{th}$ iteration, i.e. $\mathbf{J}^{(i+1)}$

Preprints (www.preprints.org) | NOT PEER-REVIEWED | Posted: 24 July 2018 doi:10.20944/preprints201807.0444.v1

can be approximated to be $\mathbf{J}^{(i)}$. Therefore, the rank one update given in (12) can be used for the Jacobian matrix in $(i+1)^{th}$ iteration.

$$\boldsymbol{J}^{(i+1)} = \boldsymbol{J}^{(i)} + \boldsymbol{X}^{(i)}\left[\boldsymbol{Y}^{(i)}\right]^{T} \tag{15}$$

In (15), $\boldsymbol{X}^{(i)}$ and $\boldsymbol{Y}^{(i)}$ are vectors whose values depend upon solution vectors and function matrix in the two consecutive iterations i.e. on $\boldsymbol{\alpha}^{(i)}$, $\boldsymbol{\alpha}^{(i+1)}$, $\boldsymbol{G}^{(i)}$, and $\boldsymbol{G}^{(i+1)}$. The Jacobian estimate formula can be derived by considering the Jacobian $\boldsymbol{J}^{(i)}$ which produces $\Delta\boldsymbol{\alpha}^{(i)}$, as given in (16)-(18).

$$\boldsymbol{J}^{(i)}\Delta\boldsymbol{\alpha}^{(i)} = -\boldsymbol{G}^{(i)} \tag{16}$$

$$\boldsymbol{\alpha}^{(i+1)} = \boldsymbol{\alpha}^{(i)} + \Delta\boldsymbol{\alpha}^{(i)} \tag{17}$$

$$\Delta\boldsymbol{G}^{(i)} = \boldsymbol{G}^{(i+1)} - \boldsymbol{G}^{(i)} \tag{18}$$

To accurately estimate the Jacobian matrix in the $(i+1)^{th}$ iteration, i.e. $\mathbf{J}^{(i+1)}$ the following two conditions should be imposed on the designed vector.

1. For a vector $\mathbf{z}$, if $\left[\Delta\boldsymbol{\alpha}^{(i)}\right]^{T} z = 0$, i.e. in the perpendicular direction of $\Delta\boldsymbol{\alpha}^{(i)}$, a new Jacobian estimate $\boldsymbol{J}^{(i+1)}$ maintains the same function vector $\boldsymbol{G}$. Both $\boldsymbol{J}^{(i)}$ and $\boldsymbol{J}^{(i+1)}$ are related to vector $\mathbf{z}$ given in (19).

$$\boldsymbol{J}^{(i)}z = \boldsymbol{J}^{(i+1)}z \tag{19}$$

2. The prediction for $\boldsymbol{J}^{(i+1)}\Delta\boldsymbol{\alpha}^{(i)}$ is same in linear expansion as for $\Delta\boldsymbol{G}^{(i)}$, i.e.

$$\Delta\boldsymbol{G}^{(i+1)} = \boldsymbol{G}^{(i)} + \boldsymbol{J}^{(i+1)}\Delta\boldsymbol{\alpha}^{(i)} \tag{20}$$

or

$$\boldsymbol{J}^{(k+1)}\Delta\boldsymbol{\alpha}^{(i)} = \Delta\boldsymbol{G}^{(i)} \tag{21}$$

Also for the normal vector z to $\Delta\boldsymbol{\alpha}^{(i)}$, the following relations are obtained given in (22)-(25);

$$\boldsymbol{J}^{(k+1)}\Delta\boldsymbol{\alpha}^{(i)} = \Delta\boldsymbol{G}^{(i)} \tag{22}$$

$$\boldsymbol{J}^{(i+1)}z = \boldsymbol{J}^{(i)}z + \boldsymbol{X}^{(i)}[\boldsymbol{Y}^{(i)}]^{T}z \tag{23}$$

$$\boldsymbol{J}^{(i+1)}z = \boldsymbol{J}^{(i)}z \tag{24}$$

$$\boldsymbol{X}^{(i)}[\boldsymbol{Y}^{(i)}]^{T}z = 0 \tag{25}$$

We can choose $\boldsymbol{y}^{(i)} = \Delta\boldsymbol{\alpha}^{(i+1)}$ because $\Delta\boldsymbol{\alpha}^{(i)}$ is perpendicular to z. After substituting in (15) and post-multiplying by $\Delta\boldsymbol{\alpha}^{(i)}$ the relationship is modified as given in (26).

$$\boldsymbol{J}^{(i+1)}\Delta\boldsymbol{\alpha}^{(i)} = \boldsymbol{J}^{(i)}\Delta\boldsymbol{\alpha}^{(i)} + \boldsymbol{X}^{(i)}[\Delta\boldsymbol{\alpha}^{(i)}]^{T}\Delta\boldsymbol{\alpha}^{(i)} \tag{26}$$

Preprints (www.preprints.org) | NOT PEER-REVIEWED | Posted: 24 July 2018 doi:10.20944/preprints201807.0444.v1

Using (21) and substituting in (15), will yield (27) and (28).

$$\Delta \boldsymbol{G}^{(i)} = \boldsymbol{J}^{(i)} \Delta \boldsymbol{\alpha}^{(i)} + \boldsymbol{X}^{(i)} [\Delta \boldsymbol{\alpha}^{(i)}]^T \Delta \boldsymbol{\alpha}^{(i)} \quad (27)$$

$$\boldsymbol{X}^{(i)} = \frac{[\Delta \boldsymbol{G}^{(i)} - \boldsymbol{J}^{(i)} \Delta \boldsymbol{\alpha}^{(i)}]}{[[\Delta \boldsymbol{\alpha}^{(i)}]^T \Delta \boldsymbol{\alpha}^{(i)}]} \quad (28)$$

Therefore, the Jacobian estimate for the next iteration can be found by (29).

$$\boldsymbol{J}^{(i+1)} = \boldsymbol{J}^{(i)} + \frac{[\Delta \boldsymbol{G}^{(i)} - \boldsymbol{J}^{(i)} \Delta \boldsymbol{\alpha}^{(i)}][\Delta \boldsymbol{\alpha}^{(i)}]^T}{[[\Delta \boldsymbol{\alpha}^{(i)}]^T \Delta \boldsymbol{\alpha}^{(i)}]} \quad (29)$$

Thus, on further simplification the approximate Jacobian estimate is given by (30).

$$\Delta \boldsymbol{G}^{(i)} - \boldsymbol{J}^{(i)} \Delta \boldsymbol{\alpha}^{(i)} = \boldsymbol{G}^{(i+1)} - \left(\boldsymbol{G}^{(i)} + \boldsymbol{J}^{(i)} \Delta \boldsymbol{\alpha}^{(i)} \right) = \boldsymbol{G}^{(i+1)} \quad (30)$$

$$\boldsymbol{J}^{(i+1)} = \boldsymbol{J}^{(i)} + \frac{1}{[[\Delta \boldsymbol{\alpha}^{(i)}]^T \Delta \boldsymbol{\alpha}^{(i)}]} [\boldsymbol{G}^{(i+1)} [\Delta \boldsymbol{\alpha}^{(i)}]^T] \quad (31)$$

The solution by iterative methods is required to generate an approximation of the set of simultaneous equations. The approximation of the solution is normally generated using the iteration sequence of vectors under considered space vector given in (32).

$$\boldsymbol{\alpha}^{(i+1)} = G[\boldsymbol{\alpha}^{(i)}] \;\; ; \; i = 0,1,2,3,\cdots \quad (32)$$

In the proposed method, the convergence criteria for the required solution are defined as in (33)-(34).

$$\max \left\| \boldsymbol{G}^{(i+1)} \right\| < \boldsymbol{\varepsilon}_1 \quad (33)$$

$$\min \frac{\left\| \boldsymbol{\alpha}^{(i+1)} - \boldsymbol{\alpha}^{(i)} \right\|}{\left\| \boldsymbol{\alpha}^{(i+1)} \right\|} < \boldsymbol{\varepsilon}_2 \quad (34)$$

Where $\varepsilon_1$and $\varepsilon_2$represent the accuracy required in the solution. The quality or effectiveness of the modulation techniques is expressed in terms of non-desirable components in the output relative to a pure sinusoidal (desired) component. For three phase system, it is expressed as given in (35).

$$\%THD = \frac{1}{V_1} \sqrt{\left[\sum_{n=1,2,3,\ldots}^{49} \left(V_{6n\pm1} \right)^2 \right]} \times 100 \quad (35)$$

Where V_1 represents the peak value of the fundamental component of line-to-line voltage and V_n represents that of n^{th} harmonics component. A systematic implementation process of the proposed method for solving the non-linear transcendental SHE equations is given in Fig. 3.

This section may be divided by subheadings. It should provide a concise and precise description of the experimental results, their interpretation as well as the experimental conclusions that can be drawn.

4. Computational and Simulation Results

For computation of switching angles Intel core i7-7500U CPU, 16 GB RAM is used and a program is written using MATLAB 2016 software. In various cases of a number of switching angles (N_s=3, 5…15) the solution trajectories of switching angles as a function of modulation index are obtained and shown in fig.(4)-(6). The minimum and maximum modulation index is set to 0 and 1,

Preprints (www.preprints.org) | NOT PEER-REVIEWED | Posted: 24 July 2018 doi:10.20944/preprints201807.0444.v1

respectively, and varied in the step of Δm=0.0001. Also, various important graphs are plotted such as a maximum error in the Non-linear system of equations given in (10), total harmonic distortion as a function of modulation, the number of iterations required to reach the convergence point set in the problem, the convergence rate for a particular modulation index and the harmonics profile at particular modulation index. Selective computational results are shown in Fig. 4 and Fig.5.

Table (1) shows the three solutions obtained by this method for Ns=5, m=0.5467. The choice of best solution is application dependent and one can choose based on minimum THD, minimum, differences in consecutive switching angles, and transition from one modulation point to another.

Table 1 Solutions for *Ns=5, m=0.5467*

	Switching angles (rad.)
1.	$\alpha_1 = 0.605, \alpha_2 = 0.776, \alpha_3 = 0.951, \alpha_4 = 1.43; \alpha_5 = 1.368$
2.	$\alpha_1 = 0.092, \alpha_2 = 0.611, \alpha_3 = 0.771, \alpha_4 = 1.371; \alpha_5 = 1.567$
3.	$\alpha_1 = 0.3503, \alpha_2 = 0.689, \alpha_3 = 0.989, \alpha_4 = 1.111; \alpha_5 = 1.539$

Figure 4(b) shows the percentage total harmonic distortion in the whole solution as a function of modulation index computed using (35). The convergence of the maximum function in (8) is shown in Fig. 4c. Figure 4d shows the convergence of the whole solutions up to a specified accuracy (~10^{-15}) for various modulation indexes. Most of the solution converges within 30 iterations which is evident from Fig. 4d.Likewise, computations are done for a large number of switching cases. Figure 5(a)-(d) shows solution trajectories for *Ns*=3, *Ns*=9, *Ns*=11 and *Ns*=13, respectively. These trajectories confirm that there are multiple solutions, unique solution and no solution in the linear range of modulation index. In case of *Ns*=15, at $m \in (0.5517, 0.7637)$ and there are three solutions at *m=0.58* and is given in Table (2). For N_s=15 the %THD lies in the range $(1.69, 2.78)$ for the entire solution obtained by the proposed method. Also, the trajectories in Fig.5, shows a similarity in the switching patterns, therefore, for higher switching angles the solution can be predicted using these trajectories and advanced mathematical techniques. A simulation model has been developed in MATLAB/Simulink to verify the computational results obtained from the proposed method. The simulation for a large number of switching angle cases have been carried out and selected results for N_s=5; and N_s=15for number of switching angles are shown in Fig. 6.Figure 6 (a) and (b) shows the solution trajectories of N_s=5 and N_s=15respectively. The spectrum phase and line voltages along with a harmonic spectrum of line voltages for m=0.84 and m=0.76is shown in Fig. 6c and 6d for N_s=5and N_s=15, respectively. The harmonics profile confirms that lower order harmonics considered for elimination are absent from the output waveforms. The next significant harmonics are of the order 17th, 19th…etc. for 11-level and 47th, 51st… etc. for 31-level case.

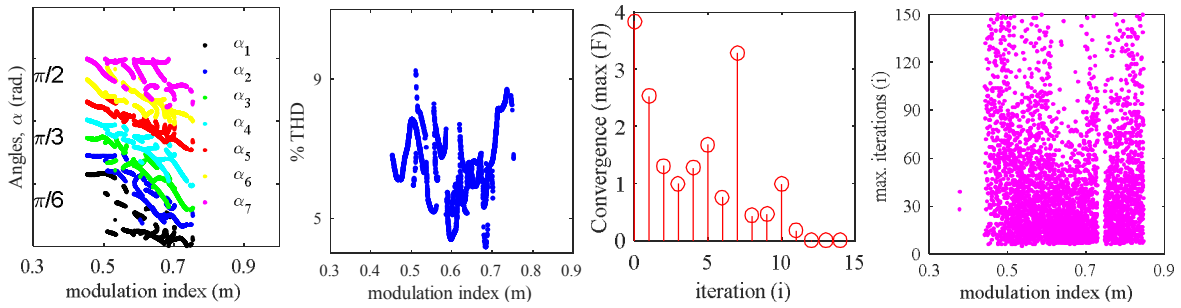

(**a**) (**b**) (**c**) (**d**)

Figure4. Computational Results for N_s=7 (15-level inverter) **(a)** Switching angles (rad.) as a function of modulation index **(b)** Percentage THD as function of modulation index **(c)** Convergence steps for m=0.53 **(d)** Maximum iterations to reach the accuracy (~10^{-15})

Preprints (www.preprints.org) | NOT PEER-REVIEWED | Posted: 24 July 2018 doi:10.20944/preprints201807.0444.v1

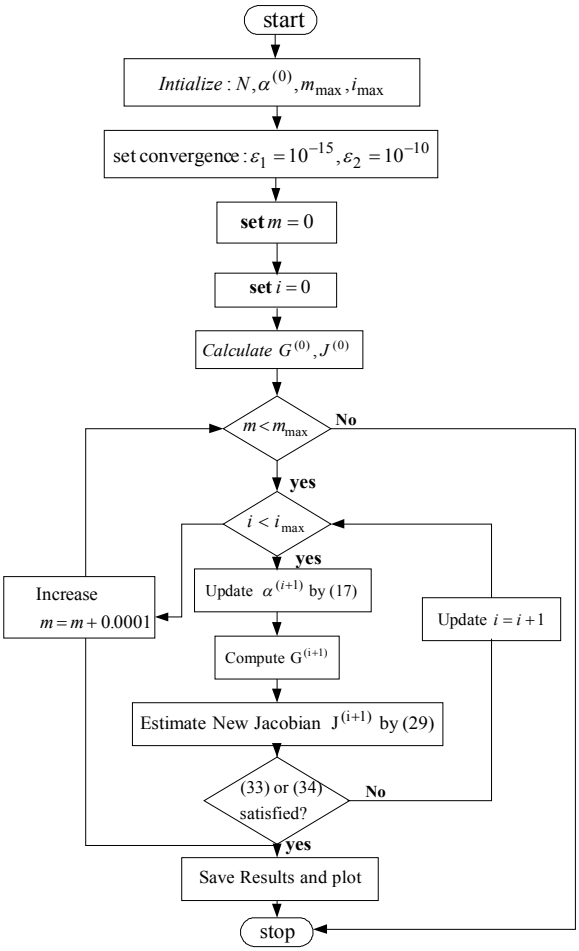

(a)

Initialize:

$$N_s,\alpha^{(0)},\varepsilon_1,\varepsilon_2,m=0,m_{\max}=1,i,i_{\max},\gamma_2=10^{-15}$$

Generate initial switching angles:

$LB=[zeros(1,N_s)];$

$UB=[pi()/2\times ones\ (1,N_s)];$

$\alpha_0=sort\ (rand(N_s,1)\times(pi()/2-.001)+.001);$

Start iterations:

$$\gamma_1=\left\|G^{(0)}\right\|$$

$$J^{(0)}=\left[\frac{\partial G(\alpha^{(0)})}{\partial\alpha}\right]$$

while $m\le m_{\max}$

while $\left[(\gamma_1>\varepsilon_1)\text{ AND }(\gamma_2>\varepsilon_2)\text{ AND }(i<i_{\max})\right]$

$$\Delta\alpha^{(i)}=-\left[J^{(i)}\right]^{-1}G^{(i)}$$

$$\alpha^{(i+1)}=\alpha^{(i)}+\Delta\alpha^{(i)}$$

$$G^{(i+1)}=G(\alpha^{(i+1)})$$

$$J^{(i+1)}=J^{(i)}+\frac{1}{[[\Delta\alpha^{(i)}]^T\Delta\alpha^{(i)}]}[G^{(i+1)}[\Delta\alpha^{(i)}]^T]$$

$$\gamma_1=\max\left\|G^{(i+1)}\right\|$$

$$\gamma_2=\min\frac{\left\|\alpha^{(i+1)}-\alpha^{(i)}\right\|}{\left\|\alpha^{(i+1)}\right\|}$$

$i=i+1$

end while

$m=m+0.0001$end while

(b)

Figure. 3. Algorithm of the proposed method

(a) Flowchart of the proposed method

(b) Pseudocode for programming

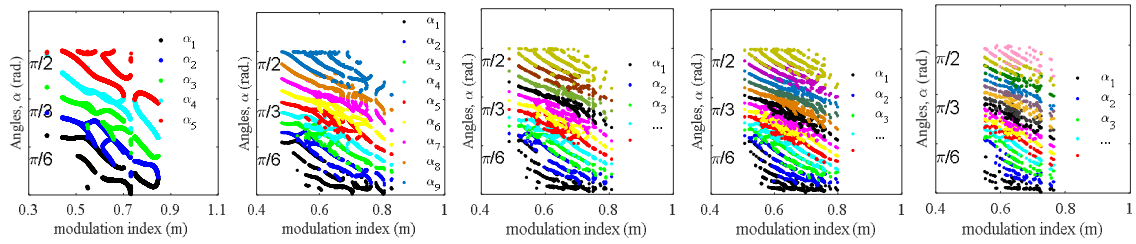

(a) (b) (c) (d)(e)

Figure5. (b) Switching angle trajectory for **(a)** Ns=5 (11-level) **(b)**Ns=9 (19-level) **(c)** Ns=11 (23-level) **(d)** Ns=13(27-level)**(e)** Switching angle trajectory for Ns=15 (31-level)

Preprints (www.preprints.org) | NOT PEER-REVIEWED | Posted: 24 July 2018 doi:10.20944/preprints201807.0444.v1

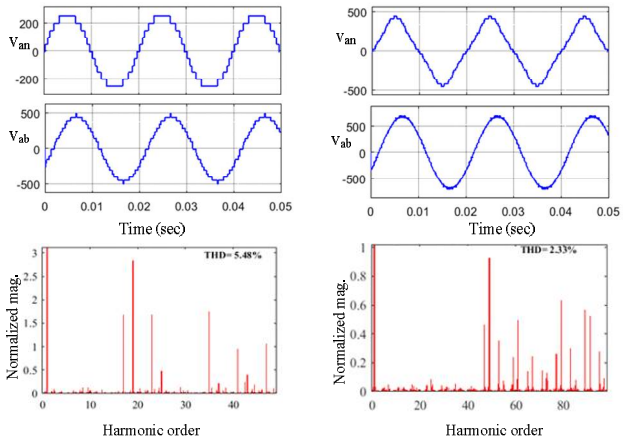

(a) **(b)**

Figure6. Simulation results**(a)** Line voltage and harmonics profile at m=0.84 for Ns=5**(b)** Line voltage harmonics profile at m=0.76 for Ns=15

Table 2 Solutions for *Ns=15, m=0.58*

Switching angles (rad.)
$\alpha_1=0.232,\alpha_2=0.570,\alpha_3=0.587,\alpha_4=0.679;\alpha_5=0.697;$ $\alpha_6=0.788,\alpha_7=0.898;\alpha_8=0.938;\alpha_9=1.013,\alpha_{10}=1.066,$ $\alpha_{11}=1.139,\alpha_{12}=1.203;\alpha_{13}=1.355;\alpha_{14}=1.442,\alpha_{15}=1.536$
$\alpha_1=0.154,\alpha_2=0.567,\alpha_3=0.589,\alpha_4=0.674;\alpha_5=0.702;$ $\alpha_6=0.782,\alpha_7=0.819;\alpha_8=0.940;\alpha_9=1.01,\alpha_{10}=1.065,$ $\alpha_{11}=1.135,\alpha_{12}=1.27;\alpha_{13}=1.352;\alpha_{14}=1.437,\alpha_{15}=1.53$
$\alpha_1=0.386,\alpha_2=0.556,\alpha_3=0.601,\alpha_4=0.719;\alpha_5=0.765;$ $\alpha_6=0.836,\alpha_7=0.877;\alpha_8=0.952;\alpha_9=0.999,\alpha_{10}=1.072,$ $\alpha_{11}=1.129,\alpha_{12}=1.203;\alpha_{13}=1.271;\alpha_{14}=1.351,\alpha_{15}=1.531$

5. Hardware setup and experimental results

A prototype is developed in the laboratory to practically validate the correctness of the switching angles computed by the proposed method. The prototype developed and the control algorithm for implementation of SHE PWM for various cases is shown in Fig. 7. The Semikron SKM100GB12T4 is used to build the H-bridge inverter. The control code is developed and implemented using Matlab/Xilinx blocks interface with FPGA VIRTEX- 5XC5VLX50T.Since the FPGA board used in the experimental work offers a clock of 50 MHz so, 20 ns time resolution of the gate signal is achieved. The dead time is not required as the two switches in the same leg never operate simultaneously. It also ensures better resolution of the output waveform and avoids any pulse dropping, in case the difference in consecutive switching angles are very small. The switching frequency of the IGBT switches of the inverter is kept at line frequency (50 Hz). The PWM gating pulses have given to gate drivers ADuM3220. For recording the harmonics profile in the output voltage waveform, a Fluke 43B single-phase power quality analyzer has been used. The harmonic content only up to 49th has been recorded since the contribution higher order harmonics in the THD is not significant.

Preprints (www.preprints.org) | NOT PEER-REVIEWED | Posted: 24 July 2018 doi:10.20944/preprints201807.0444.v1

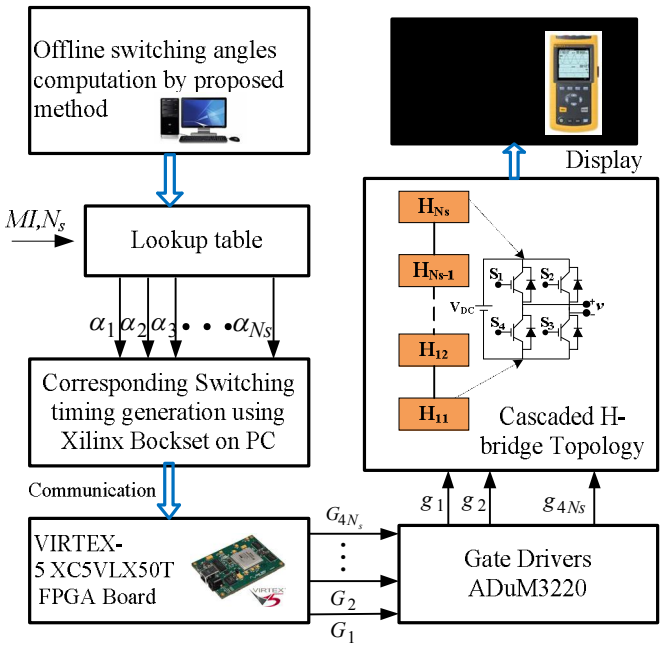

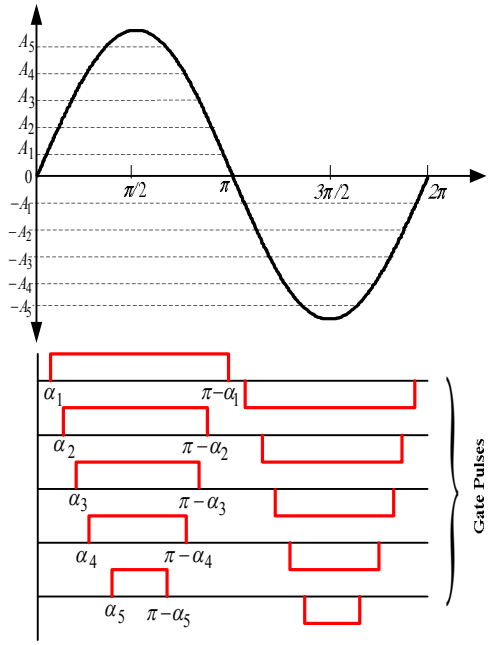

(a) (b)

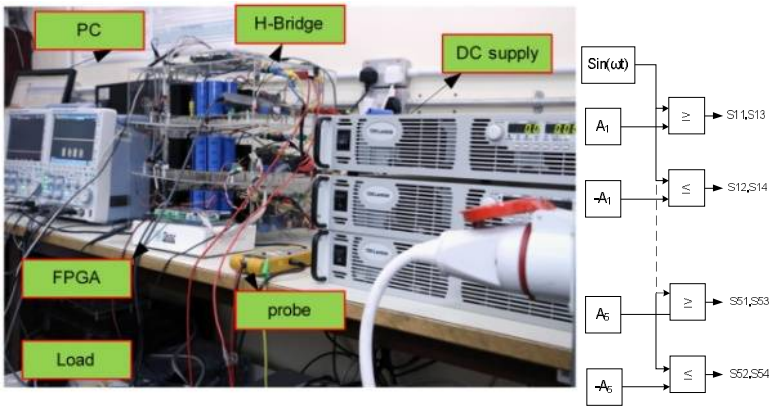

(c) (d)

Preprints (www.preprints.org) | NOT PEER-REVIEWED | Posted: 24 July 2018 doi:10.20944/preprints201807.0444.v1

Figure.7 Hardware setup and Experimental procedure**(a)** Hardware schematic **(b)** Gating pulse generation**(c)** Actual prototype developed in the laboratory**(d)** Logics to generate gating pulses

For 7-level and 11-level cascaded H-bridge case, the experiments have been carried out using the developed prototype. The experimental data are given in Table (3). The sine magnitude of the switching angles computed in the previous section is stored in the lookup table. This stored value as per modulation index fed switching instants and compared with a sinusoidal waveform to produce gating pulses as shown in Fig. 7b and 7d. The selected results for *m=0.747* and *m=0.836* have been shown for 7-level and 11- level cases in Fig.8. The voltage spectrum shows that the targeted harmonics for elimination i.e. 5^{th} 7^{th} and 5^{th} 7^{th}, 11^{th}, 13^{th} are absent in the output voltage waveform respectively.

Table 3 Experimental parameters

Ns	f_{sw} (Hz)	Vdc
3	50	90 V
5	50	40 V

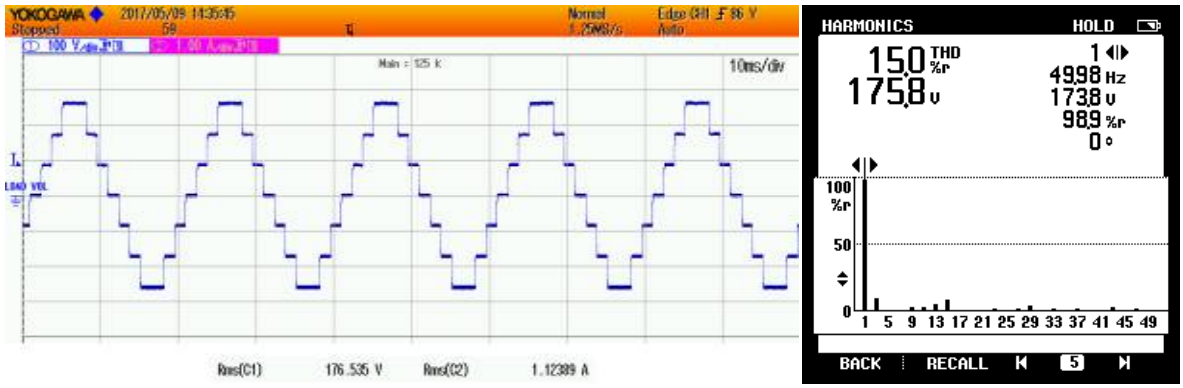

(a)

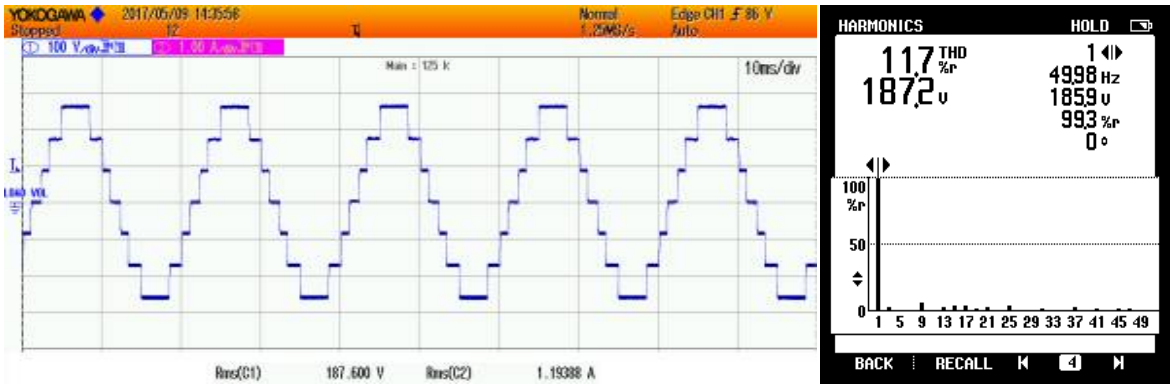

(b)

Preprints (www.preprints.org) | NOT PEER-REVIEWED | Posted: 24 July 2018 doi:10.20944/preprints201807.0444.v1

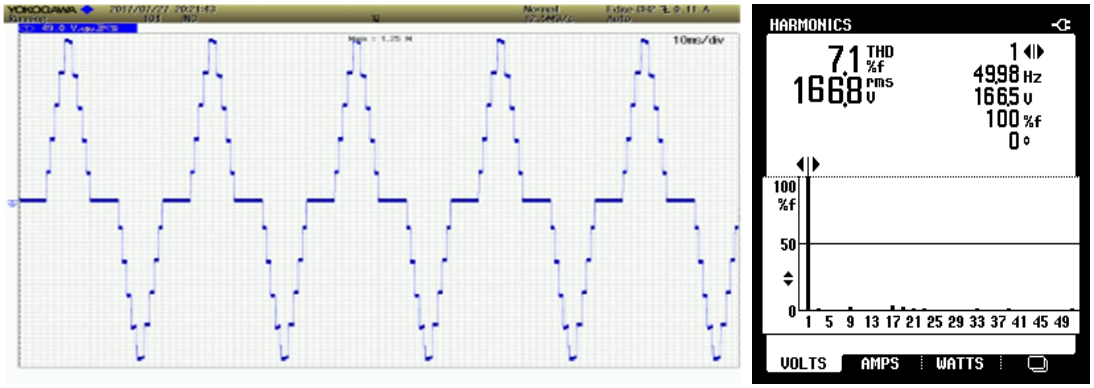

(c)

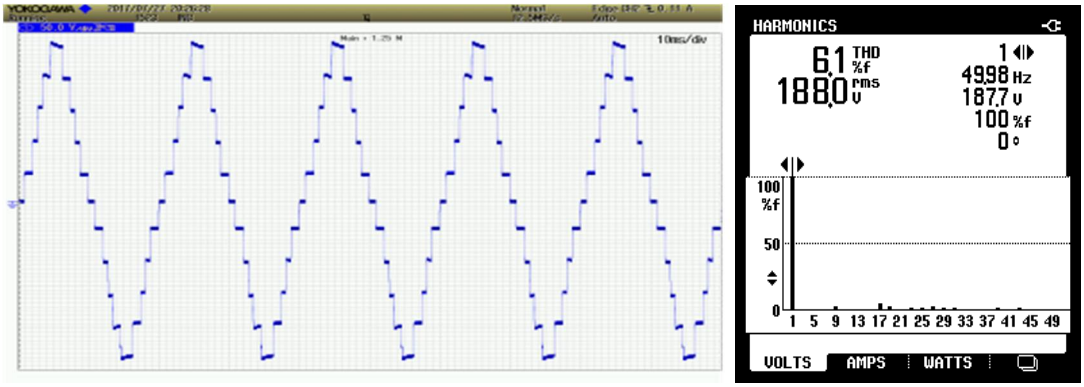

(d)

Figure.8 Hardware results**(a)** Phase voltages at m=0.505 for Ns=3**(b)** Phase voltages at m=0.550 for Ns=3**(c)** Phase voltages at m=0.747 for Ns=5**(d)** Phase voltages at m=0.836 for Ns=5

5. Conclusion

In this paper, a novel Jacobian estimation based iterative method is proposed for the computation of switching angles in the selective harmonics elimination problem. Since the computation of the Jacobian is avoided in each iteration, the speed of computation is fast. Moreover, the singularity problem associated with the inverse of the Jacobian matrix evaluation is also avoided. It makes the proposed method more suitable for computation of a large number of switching angles in SHE PWM and hence higher stepped waveform. Moreover, the fast computational speed allows taking a very small step increment for modulation index and it ensures multiple solutions at various modulation indexes. The non-triplen lower order odd harmonics are considered for elimination from the output waveform. The proposed technique has been successfully implemented for switching angles from three to fifteen or from seven levels stepped waveform to 31 levels stepped waveforms. In the different range of modulation indices, different numbers of solutions are found. The %THD for all the cases and solutions is also computed and reported. Selective computational and simulation results are given for 11-level and 31-level. A prototype is also developed and practical results are provided for 7-level and 11-level to validate the computational results.

Author Contributions: All authors contributed equally to the final presented research article.

Funding: This paper was made possible by NPRP grant # X-033-2-007 from the Qatar National Research Fund (a member of Qatar Foundation). The statement made herein are solely the responsibility of the authors.

Conflicts of Interest: The authors declare no conflict of interest.

References

1. Rodríguez, J., Lai, J., and Peng, F., 'Multilevel Inverters : A Survey of Topologies, Controls, and Applications', 2002, **49**, (4), pp. 724–738.
2. Malinowski, M., Gopakumar, K., Rodriguez, J., Perez, A., 'A survey on cascaded multilevel inverters',*IEEE Trans. Ind. Electron.*, 2010, **57**, (7), pp. 2197–2206.
3. Kouro, S., Malinowski, *M., Gopakumar*, K., et al., 'Recent Advances and Industrial Applications of Multilevel Converters', *IEEE Trans. Ind. Electron.*, 2010, **57**, (8), pp. 2553–2580.
4. Steczek, M., Chudzik, P., and Szelag, A., 'Combination of SHE and SHM - PWM techniques for VSI DC-link current harmonics control in railway applications',2017, *IEEE Trans. Ind. Electron.*, **46**, (6), pp. 2155–2170.
5. S. S. Lee, B. Chu, N. Rumzi, N. Idris, and, "Switched-Battery Boost-Multilevel Inverter with GA Optimized SHEPWM for Standalone Application" ,2015, *IEEE Trans. Ind. Electron.*, **46**, (8).
6. Imarazene, K., Chekireb, H., Berkouk, E.M.: 'Selective harmonics elimination PWM with self-balancing DC-link in photovoltaic 7-level inverter'*Turkish J. Electr. Eng. Comput. Sci.*, 2016, **24**, (5), pp. 3999–4014.
7. Zabaleta, M., Burguete, E., Madariaga, D., et al., 'LCL grid filter design of a multimegawatt medium-voltage converter for offshore wind turbine using SHEPWM modulation'*IEEE Trans. Power Electron.*, 2016, **31**, (3), pp. 1993–2001.
8. B. Wu, *High-power converters and ac drives*. Wiley-IEEE press, 2006.
9. Lin, L., Lin, Y., He, Z., et al., 'Improved Nearest-Level Modulation for a Modular Multilevel Converter With a Lower Submodule Number'*IEEE Trans. Power Electron.*, 2016, **31**, (8), pp. 5369–5377.
10. Dahidah, M., Konstantinou, G., and Agelidis, V., 'A Review of Multilevel Selective Harmonic Elimination PWM: Formulations, Solving Algorithms, Implementation and Applications', *IEEE Trans. Power Electron.*, 2015, **30**, (8), pp. 4091–4106.
11. Yang, K., Zhang, Q., Zhang, J., et al., 'Unified selective harmonic elimination for multilevel converters', IEEE Trans. Power Electron., 2017, 32, (2), pp. 1579–1590
12. J. G. H Abu-Rub, A Iqbal, *High performance control of AC drives with MATLAB/Simulink models*. Wiley , 2012.
13. Konstantinou, G., Pou, J., Capella, G.J., Song, K., Ceballos, S., Agelidis, V.G.: 'Interleaved Operation of Three-Level Neutral Point Clamped Converter Legs and Reduction of Circulating Currents under SHE-PWM'*IEEE Trans. Ind. Electron.*, 2016, **63**, (6), pp. 3323–3332.
14. Luiz, A.S.A., Filho, B.J.C.: 'A new design of selective harmonic elimination for adjustable speed operation of AC motors in mining industry'. IEEE Int. Conf. Applied Power Electronics Conf. Exposition (APEC), March 2017, pp. 607–614.
15. Flourentzou, N., and Agelidis, V., 'Multimodule HVDC system using SHE-PWM with DC capacitor voltage equalization,*IEEE Trans. Power Deliv.*, 2012, **27**, (1), pp. 79–86.
16. S. R. Pulikanti, G. Konstantinou, and V. G. Agelidis, "DC-link voltage ripple compensation for multilevel active-neutral-point- clamped converters operated with SHE-PWM," *IEEE Trans. Power Deliv.*,2012, **27**, (4), pp. 2176–2184.
17. Mei, J., Xiao, B., Shen, K., et al., 'Modular multilevel inverter with new modulation method and its application to photovoltaic grid-connected generator', 2013*IEEE Trans. Power Electron.*, **28**,

(11), pp. 5063–5073.

18. Filho, F., Tolbert,Cao, L., and Ozpineci, B., 'Real-time selective harmonic minimization for multilevel inverters connected to solar panels using artificial neural network angle generation', 2011 *IEEE Trans. Ind. Appl.*, **47**, (5), pp. 2117–2124.
19. Y. Gopal , D. Birla and M. Lalwani."Selected Harmonic Elimination for Cascaded Multilevel Inverter Based on Photovoltaic with Fuzzy Logic Control Maximum Power Point Tracking Technique", *MDPI-Technologies***2018**, 6, 1-17.
20. Konstantinou, G., Ciobotaru, M., and Agelidis, V., 'Selective harmonic elimination pulse-width modulation of modular multilevel converters', *IET Power Electron.*, 2013, **6**, (1), pp. 96–107.
21. Nibouche, M., Bouchhida, O., and Makhlouf, B., 'Design, analysis and implementation of real-time harmonics elimination: a generalised approach', *IET Power Electron.*, 2014, **7**, (9), pp. 2424–2436.
22. Enjeti, P., Ziogas, P., and Lindsay, J., 'Programmed PWM tech- niques to eliminate harmonics: a critical evaluation', *IEEE Trans. Ind. Appl.*, 1990, **26** , (2) pp. 302-316.
23. Haw, L., Dahidah, M., and Almurib, H., 'SHE-PWM cascaded multilevel inverter with adjustable DC voltage levels control for STATCOM applications', *IEEE Trans. Power Electron.*, 2014, **29**, (12), pp. 6433–6444.
24. Mohammed Al-Hitmi, Salman Ahmad, Atif Iqbal, SanjeevikumarPadmanaban, "Selective Harmonic Elimination in a Wide Modulation Range Using Modified Newton – Raphson Multilevel Inverter," *MDPI, energies*, vol. 11, no. 458, pp. 1–16, 2018.
25. Lou, H., Mao, C., Wang, D., Lu, J., and Wang, L., 'Fundamental Modulation Strategy with Selective Harmonic Elimination for Multilevel Inverters', IET Power Electronics, 2014, **7**, (8), pp. 2173-2181.
26. Konstantinou,Dahidah, M., and Agelidis, V.,'Solution trajectories for selective harmonic elimination pulse-width modulation for seven-level waveforms: analysis and implementation', 2012, IET Power Electron., **5**, (1), pp. 22-30.
27. Salam, Z., Majed, A., and Amjad, A., 'Design and implementation of 15-level cascaded multi-level voltage source inverter with harmonics elimination pulse-width modulation using differential evolution method',*IET Power Electron.*, 2015, **8**, (9), pp. 1740–1748.
28. Filho. F., Maia, H., Mateus, T., et al., 'Adaptive selective harmonic minimization based on ANNs for cascade multilevel inverters with varying DC sources'*IEEE Trans. Ind. Electron.*, 2013, **60**, (5), pp. 1955–1962.
29. Aguilera, R., Lezana, P., Konstantinou, G., et al., 'Closed-loop SHE-PWM technique for power converters through Model Predictive Control' 2015, in Industrial Electronics Society, IECON-41st Annual Conference of the IEEE, Yokohama, Japan, pp. 005 261–005 266.
30. Ahmed, M., Sheir, A., Orabi, M. 'Real Time Solution and Implementation of Selective Harmonic Elimination of Seven-Level Multilevel Inverter'*IEEE J. Emerg. Sel. Top. Power Electron.*, 2017,.**5**, (4), pp. 1700-1709.
31. Balasubramonian, M. and Rajamani, V., 'Design and Real-Time Implementation of SHEPWM in Single- Phase Inverter Using Generalized Hopfield Neural Network', IEEE Transactions on Industrial Electronics, 2014, **61**, (11), pp. 6327-6336.
32. Dagan, K., and Rabinovici, R., 'Criteria-based modulation for multilevel inverters', *IEEE Trans. Power Electron.*, 2015, **30**, (9), pp. 5009–5018.

33. Kato. T, "Sequential Homotopy-Based Computation of Multiple Solutions for Selected Harmonic Elimination in PWM Inverters," *IEEE Trans. Cicuits Syst. Fundam. theory Appl.*, 1999, **46**, (5), pp. 586–593.
34. Buccella, C., Cecati, C., Cimoroni, M., and Razi, K., 'Analytical method for pattern generation in five-level cascaded H-bridge inverter using selective harmonic elimination',*IEEE Trans. Ind. Electron.*, 2014, **61**, (11), pp. 5811–5819.
35. Swift. F and Kamberis, A., 'A New Walsh Domain Technique of Harmonic Elimination and Voltage Control in Pulse Width Modulated Inverters',*IEEE Trans. Power Electron.*, 1993, **8**, (2), pp. 170–185.
36. Chiasson, J., Tolbert, L., McKenzie, K., and Du, Z., 'Control of a multilevel converter using resultant theory',*IEEE Trans. Control Syst. Technol.*, 2003,**11**, (3), pp. 345–354.
37. K. Yang, Z. Yuan, R. Yuan, W. Yu, J. Yuan, and J. Wang, "A Groebner Bases Theory Based Method for Selective Harmonic Elimination," *IEEE Trans. Power Electron.*, 2015, **30**, (12), pp. 6581–6592.
38. Ozpineci, B., Tolbert, L., and Chiasson, J.,'Harmonic Optimization of Multilevel Converters Using Genetic Algorithms', *IEEE Power Electronics letters*, 2005, **3**, (3), pp. 92–95.
39. Ray, R., Chatterjee, D., and Goswami, S., 'Harmonics elimination in a multilevel inverter using the particle swarm optimisation technique', *IET Power Electron.*, 2009, **2**,(6), p. 646.
40. Kavousi, A., Vahidi, B., Salehi, R.,et al., 'Application of the bee algorithm for selective harmonic elimination strategy in multilevel inverters', *IEEE Trans. Power Electron.*, 2012, **27**, (4), pp. 1689–1696.
41. Sundareswaran, K., Jayant, K., and Shanavas, T., 'Inverter Harmonic Elimination Through a Colony of Continuously Exploring Ants' *IEEE Trans. Ind. Electron.*, 2007, **54**, (5), pp. 2558–2565.
42. Heidari, Y., Jabbarvaziri, F., Niknam Kumle, A., et al., 'Application of memetic algorithm for selective harmonic elimination in multi-level inverters', *IET Power Electron.*, 2015, **8**, (9), pp. 1733–1739.
43. Kundu, S., Burman, A.D., Giri, S.K., Mukherjee, S., Banerjee, S.: 'Comparative study between different optimisation techniques for finding precise switching angle for SHE-PWM of three-phase seven-level cascaded H-bridge inverter', *IET Power Electron.*, 2018, **11**, (3), 600-609.